Quaternary Science Reviews 30 (2011) 469–479

Contents lists available at ScienceDirect

Quaternary Science Reviews

journal homepage: www.elsevier.com/locate/quascirev

The impact of varying ice sheets and greenhouse gases on the intensity and timing of boreal summer monsoons

S.L. Weber [a,b,*], E. Tuenter [a,b]

[a] Royal Netherlands Meteorological Institute (KNMI), Climate and Seismology, P.O. Box 201, 3730 AE De Bilt, The Netherlands
[b] Faculty of Geosciences, Utrecht University, The Netherlands

ARTICLE INFO

Article history:
Received 7 December 2009
Received in revised form
2 December 2010
Accepted 8 December 2010
Available online 3 January 2011

Keywords:
Orbital forcing
Monsoons
Model study
Late Quaternary

ABSTRACT

Climate models, forced only with insolation, indicate that boreal summer monsoons respond to orbital forcing with a zero phase both at the precession and obliquity bands. Discrepancies exist among data with respect to the timing of the response. Some late Pleistocene monsoon records show small lags of 2–3 kyr, close to model results, while many others show considerably longer lags of 5–8 kyr. It has been hypothesized that such lags arise from factors that were, up till now, not included in the modelling experiments, namely variations in glacial-age boundary conditions.

Here we address this issue using long, time-dependent climate simulations that do include varying ice sheets and greenhouse gas concentrations. Inclusion of these additional forcings introduces a small peak in the monsoon spectra at the 100 kyr period, while monsoon variance remains dominated by precession with a smaller contribution from obliquity. At the precession band orbital forcing remains the dominant control, with lags close to zero. At the obliquity band varying ice sheet and greenhouse gases explain most of the simulated African and Indian monsoon variance, with orbital forcing playing a minor role. For the East Asian monsoon orbital forcing remains dominant. As a result the simulated obliquity phase of different monsoon systems lies between summer insolation maxima and ice minima/greenhouse gas maxima, with a lag that varies with distance to the Eurasian ice sheet.

1. Introduction

Data unambiguously show that boreal summer monsoons vary in response to changes in insolation caused by changes in the Earth's orbit. However, the causal links between the orbital forcing and climate are as yet not clear and much research has been devoted to establish such links using a range of models and experimental set-ups. The earliest modelling experiments were done with atmosphere-only models for specific time periods like the early Holocene (Kutzbach, 1981). This type of experiment typically shows that stronger summer insolation results in an enhanced seasonal cycle of temperature over the Northern Hemisphere (NH) continents, a stronger land-sea temperature contrast and associated intensified low-level convergence into the monsoon lows over northern Africa and Eurasia, although details can differ among models (Joussaume et al., 1999). The inclusion of ocean and vegetation feedbacks modifies the spatial response pattern of regional monsoon systems and their strength. Nevertheless, the latest Atmosphere/Ocean (AO) and Atmosphere/Ocean/Vegetation (AOV) experiments basically show similar responses as described earlier for atmosphere-only models (Braconnot et al., 2007).

These 'snap-shot' experiments for specific time periods have recently been complemented by transient experiments that simulate the evolutionary response of the monsoon systems to the time-varying orbital forcing. Such experiments allow to establish phase relationships between monsoons and the only forcing included - insolation. This has showed that boreal summer monsoons vary approximately in phase with peak summer insolation, both in an AOV intermediate-complexity model (Tuenter et al., 2005) and an AO General Circulation Model (GCM; Kutzbach et al., 2008). Wang et al. (2008) showed in a cave record a small phase lag for the late Pleistocene, close to these modelling results. Also, Lourens et al. (1996) found lags of ca 3 kyr. However, other records indicate considerably longer lags of up to 8 kyr (Wang et al., 2005; Clemens et al., 2010 and references therein). Without going into all the issues related to the precise dating and the interpretation of the records (see, for example, Clemens et al., 2010) that may play a role in this divergence among data, we note here that addressing model-data

* Corresponding author. Royal Netherlands Meteorological Institute (KNMI), Climate and Seismology, P.O. Box 201, 3730 AE De Bilt, The Netherlands. Tel.: +31 30 2206756; fax: +31 30 2202570.
E-mail address: weber@knmi.nl (S.L. Weber).

0277-3791/$ – see front matter © 2010 Elsevier Ltd. All rights reserved.
doi:10.1016/j.quascirev.2010.12.009

discrepancies is hindered by the experimental set-up used to date. Model experiments have been done with orbital forcing and present-day boundary conditions, whereas the majority of data records represent the (late) Quaternary which is characterised by glacial cycles. For this period varying ice sheets and greenhouse gas concentrations are a dominant feature of the climate system.

Here we take the next step and present results from transient model experiments that do include, for the first time, varying ice-sheets and greenhouse-gas concentrations. Simulations are done for the period 650–0 kyr BP (thousands of years Before Present) with a coupled AOV model of intermediate-complexity. The prescribed ice-sheet variations are based on marine benthic δ^{18}O (Lisiecki and Raymo, 2005), which has been split into contributions from ice-sheet volume and deep-ocean temperature using an inverse ice-sheet/climate model (Bintanja et al., 2005). Variations in greenhouse gas concentrations are obtained from ice cores from the Antarctic Dome C (Lüthi et al., 2008; Loulergue et al., 2008), together with other sources for the most recent years (Robertson et al., 2001). The orbital forcing is computed following (Laskar et al., 2004). The main research question is how the inclusion of ice and greenhouse gas feedbacks modifies the intensity of the monsoons and their timing with respect to the orbital forcing.

2. The model, forcings and experimental set-up

2.1. The intermediate-complexity AOV model

We use the coupled model of intermediate-complexity CLIMBER-2 (for CLIMate and BiosphERe, version 3, Petoukhov et al., 2000), that is suitable for very long (paleo) simulations due to its fast turnaround time. The model consists of a statistical-dynamical atmospheric component, a 3-basin zonally averaged ocean component including sea ice and a terrestrial vegetation component. This version of the model does not contain an ice sheet component. The atmosphere resolves the large-scale flow that arises due to spatial temperature gradients. It parameterises transports due to synoptic-scale variations in a sophisticated manner (Petoukhov et al., 2000), but it does not contain the weather events themselves. As a consequence, the model lacks variations in the timescale range from days to decades. The atmosphere has a resolution of 10° in latitude and approximately 51° in longitude.

Results of CLIMBER-2 compare favorably with observations of the modern climate (Petoukhov et al., 2000). The model is also successful in simulating cold climates like the Last Glacial Maximum (LGM; Ganopolski et al., 1998a) as well as orbitally forced warm periods like the mid-Holocene (Ganopolski et al., 1998b). The sensitivity of the NH summer monsoons in CLIMBER-2 to changing conditions like vegetation and solar constant is comparable to that of higher resolution GCMs (Ganopolski et al., 2001). Also the strength of the NH monsoons during the mid-Holocene lies within the range of GCMs (Braconnot et al., 2002). The model thus adequately represents many aspects of reconstructed large-scale climatic change. It has been used earlier for orbitally forced transient simulations of boreal monsoons during the Holocene (Claussen et al., 1999) and an extreme eccentricity cycle of the late Pleistocene (the period 280–130 kyr BP; Tuenter et al., 2005).

2.2. The waxing and waning of ice sheets

Ice-sheet variations are derived from a simulation with a 3-dimensional ice sheet model, coupled to a model of deep-ocean temperature (Bintanja et al., 2005). This model is forced by marine benthic δ^{18}O (Lisiecki and Raymo, 2005), which is assumed to be governed by NH ice-sheet storage as well as local deep-water temperature. Applying the model in inverse mode results in timeseries of the North American and Eurasian ice-sheet volumes. These have subsequently been translated into a surface area and height, which are the necessary boundary conditions for the climate simulations.

For the surface area we used as a reference the ICE-5G ice distribution from the LGM until present (Peltier, 2004), set on the spatial grid of CLIMBER-2 (Ganopolski et al., 1998a). The North American ice sheet is mainly located on the continental mainland, with a smaller part in western Alaska and on the Bering Strait shelf. In Eurasia ice was present during the LGM (and earlier glacial periods) on the land north of 60 °N which was exposed due to the lowered sea level. In the standard representation of the present-day Earth geography in CLIMBER-2 there is hardly any land there. Therefore, the land fractions of northern Eurasian gridboxes were increased for the experiment that includes varying ice sheets. A test simulation, including the increased land fractions but with the present-day ice-sheet distribution, was compared to a standard control simulation in order to examine the possible impact of the modified land–sea distribution. Over the gridboxes with the new land fractions the climate differs from the control simulation, but over the other gridboxes the results were not significantly changed. From this we conclude that increasing the land fractions in a few gridboxes does not significantly affect the climate. We use either the extended fractions or the standard geography, depending on whether varying ice sheets are included or not. Land fractions do not vary during the simulations.

The time-varying area of each ice sheet is now determined as follows. ICE-5G gives a reconstruction every 1000 yrs from 21 kyr BP until present. The ice fractions, set on the CLIMBER grid, were linearly interpolated in time to obtain annual resolution. The ice sheet area at every ice-covered gridbox was then computed by multiplying the ice fraction with the land fraction and the area of that gridbox. Finally, the ice sheet areas were extrapolated back to 650 kyr BP using the ice sheet volumes. In this way, the total area (Fig. 1) as well as the area for each ice sheet includes the same temporal behaviour and the same (orbital) periods as the volumes reconstructed by the 3-D ice sheet model. For the Eurasian ice sheet the 3-D model simulates larger volumes during earlier glacials than during the LGM (not shown). Because there is no information about the ice sheet areas during these glacials, the areas were set at the LGM value resulting in some 'cutoffs' (Fig. 1). This does not apply to the North American ice sheet because the 3-D model simulates the largest volume for the LGM.

From the known areas and volumes the height for every gridbox can now be determined. We let the North American and Eurasian ice sheets have height H_{am} and H_{eur} at their central gridboxes. The ratios between the height at the central gridbox and those at adjacent gridboxes were taken from the ICE-5G reconstruction for the LGM to present. As for the ice sheet areas, the ratios were extrapolated back to 650 kyr BP using the volumes. For every gridbox and every year the relative heights and the areas of ice cover are now known. From this the absolute heights follow from the known area and volume of each ice sheet.

For our purpose of studying boreal summer monsoon variations, surface albedo is likely the most relevant aspect of ice-sheet variations. Albedo variations strongly modify the climate, directly affecting the response to insolation variations. Such a local thermodynamic response is especially important in summer, whereas ice-sheet related variations in orography mainly play a role for the wintertime climate response which is strongly determined by dynamical processes (Hall et al., 2005).

During the (prescribed) waxing and waning of the ice sheets there is no transport of water from the oceans to the ice sheets and vice versa. In other words, the sea level in the model does not change during the glacial cycles. The height and surface area of

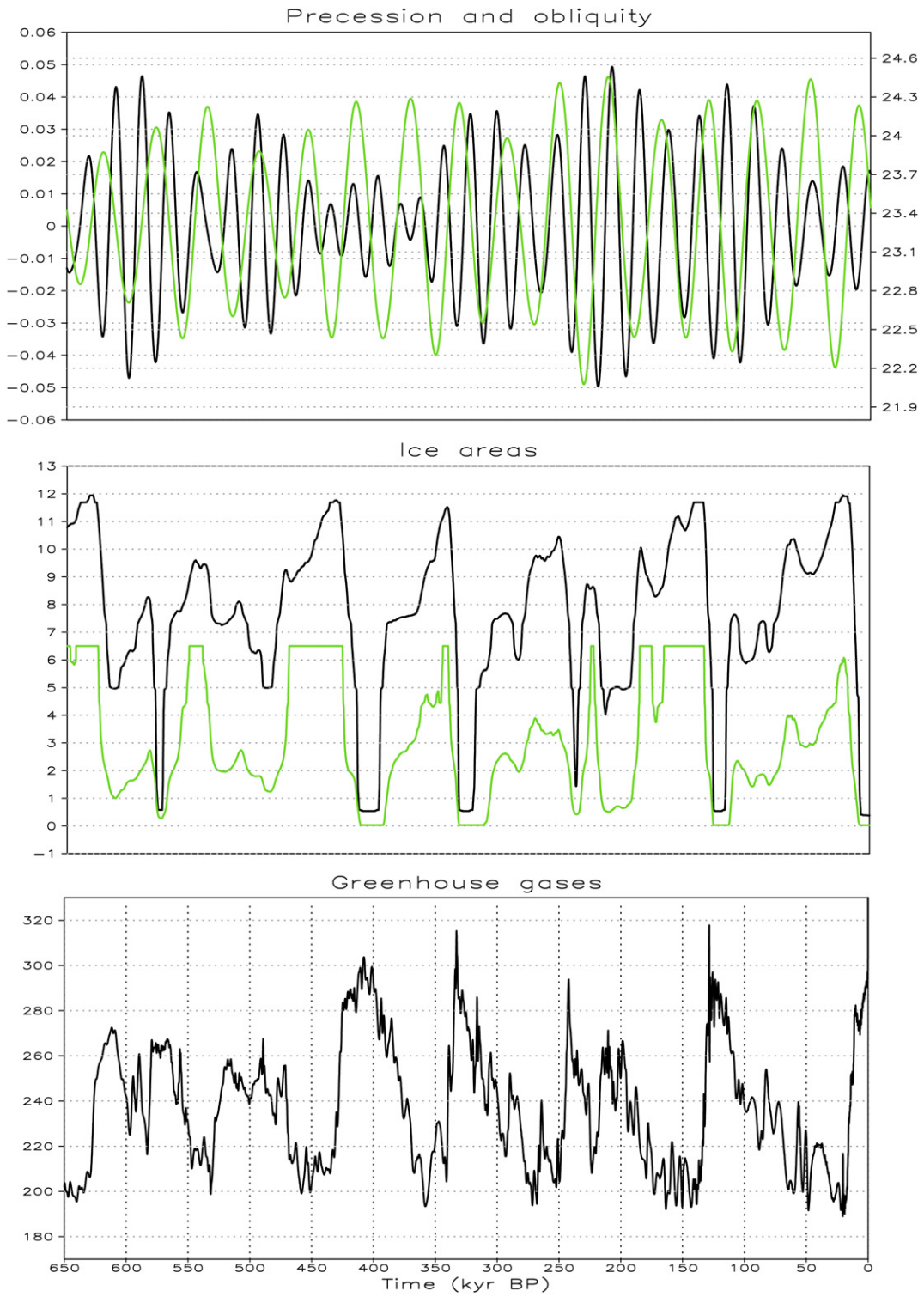

Fig. 1. Timeseries of the precession (black, left axis) and obliquity (green, right axis) parameters, ice areas of the American (black) and Eurasian (green) ice sheets (in 10^6 km^2) and total greenhouse gas forcing (that is, CO_2 and CH_4 combined; in ppmv). (For interpretation of the references to colour in this figure legend, the reader is referred to the web version of this article).

Greenland and Antarctica as well as small glaciers are kept at present-day values in all runs.

2.3. Variations in greenhouse gases

The used concentrations of CO_2 and CH_4 prior to ~500 yr BP are from the Antarctic ice core EPICA Dome C with the EDC3 timescale (Lüthi et al., 2008; Loulergue et al., 2008). For the last ~500 yrs we used values from several sources (Robertson et al., 2001). The sampling frequencies for both CO_2 and CH_4 are irregular in time and differ for both gases. We interpolated both records to obtain annual values using cubic spline interpolation. Because radiation in CLIMBER-2 only depends on CO_2 and not on other greenhouse gases, we translated the CH_4 record into an equivalent CO_2 record.

Here we use the fact that one molecule CH_4 is 21 times more effective in absorbing longwave radiation than a molecule CO_2 (Shine et al., 1990). At the same time CH_4 concentrations (measured in parts per billion by volume) are lower and vary by a much smaller amount than CO_2 concentrations (measured in parts per million by volume). The combined record of 'equivalent' CO_2 (or the total greenhouse gas forcing) follows by adding the two records, taking their relative effectiveness into account (Fig. 1).

2.4. Experimental set-up

With CLIMBER-2 we performed two different transient simulations for the interval from 650 kyr BP to present. The first experiment (simulation O) uses only orbital forcing, while ice sheets and greenhouse gas concentrations are kept fixed at pre-industrial values. This experiment is an extension of the experiment PTV described in Tuenter et al. (2005). The orbital parameters (i.e. eccentricity, precession and obliquity) for the simulations were obtained from Laskar et al. (2004). Precession is defined as $e \sin \tilde{\omega}$ with e being the eccentricity of the Earth's orbit and $\tilde{\omega}$ the angle between the vernal equinox and perihelion (measured counter clockwise). The second experiment (simulation OIG) uses varying NH ice sheets and varying greenhouse gas concentrations, in addition to the orbital forcing.

Initial states for each experiment were obtained by performing a 5000-yr spin-up run using the appropriate fixed boundary conditions for 650 kyr BP. The results will be shown as averages over 100 years, as the orbital periods that are of interest here are much longer. All boreal monsoon systems have strong precipitation in CLIMBER-2 in the months June to August, for some systems extending into September. In the following we will therefore analyse results for June–July–August (JJA). As NH summer insolation is maximum for minimum precession (boreal summer solstice in perihelion) and maximum obliquity, we will compute phase relationships with zero phase set at minimum precession and maximum obliquity.

3. Monsoon response to orbital forcing

Timeseries of the forcing factors used in run O and run OIG are shown in Fig. 1. The spectra of ice sheets and greenhouse gases (Fig. 2) exhibit a strong 100 kyr component. There is also a clear obliquity component in the ice-sheet variations, together with a weaker precession component. The total greenhouse gas forcing (CO_2 and CH_4 combined) shows a weak obliquity component, while precession is almost absent. The latter component is more clearly present in CH_4 itself, but variations in CH_4 are too small to have a large impact on the combined spectrum. Ice-sheet area reaches its minimum at a 4.3 kyr lag after NH summer insolation maxima at the precession band, with a correlation $\rho = -0.84$. At the obliquity band there is a 7.1 kyr lag, with $\rho = -0.94$. Greenhouse gases do not correlate with precession, while $\rho = 0.93$ with lag 6.2 kyr at the obliquity band. They are reasonably coherent ($\rho = -0.68$) with ice area at the precession band with a lag of 0.3 kyr. At the obliquity band there is an even higher coherence ($\rho = -0.97$), with a 1.1 kyr lag.

CLIMBER-2 simulates an intensification of boreal summer monsoons in response to an increase in NH summer insolation. The signal is very clear for the African (the gridbox centered at 11 °E and 15 °N), Indian (63 °E and 25 °N) and East Asian (114 °E and 35 °N) monsoon systems (Fig. 3) and only weakly present for the American monsoons. Therefore, we focus here on the African/Asian region. We separately consider the precession and obliquity bands for the whole period 650–0 kyr BP by band-pass filtering the forcings and model output for periods between 18 and 24 kyr (precession) and

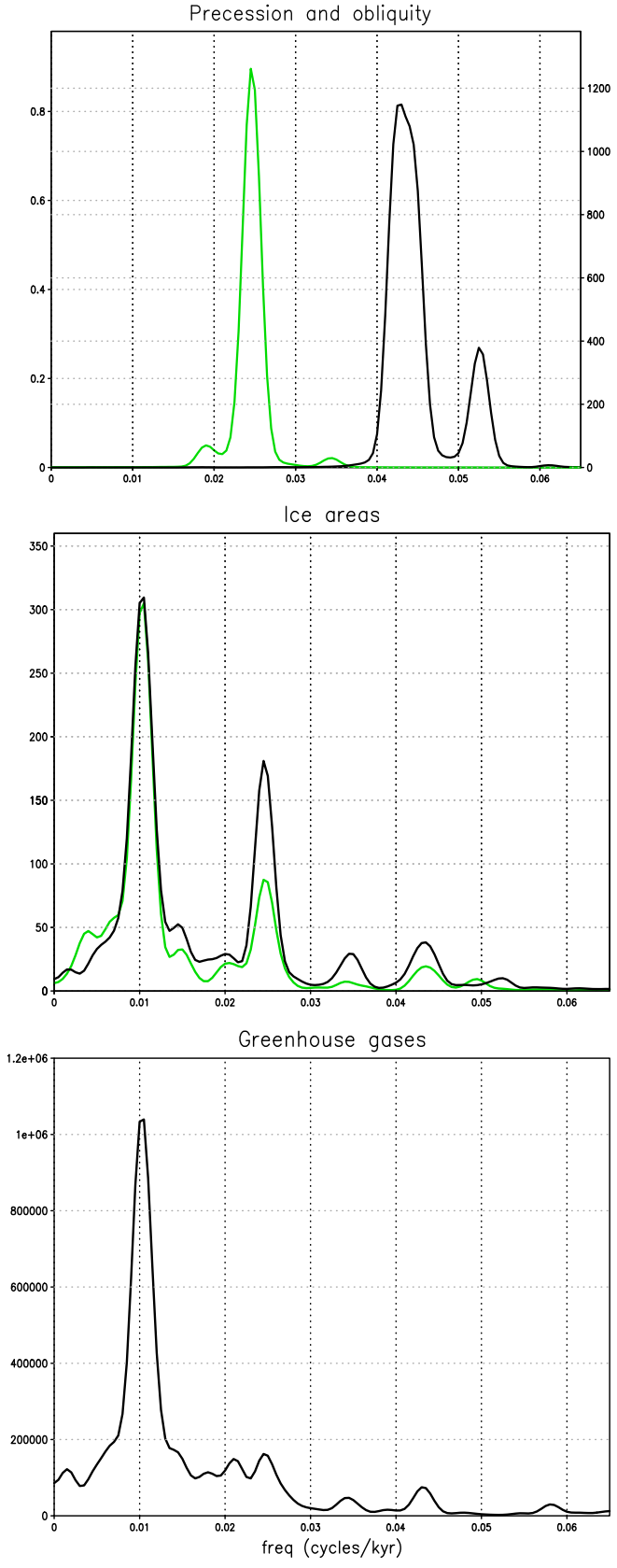

Fig. 2. Spectra of the precession (black, left axis) and obliquity (green, right axis) parameters, the American (black) and European (green) ice areas and the total greenhouse gas forcing. (For interpretation of the references to colour in this figure legend, the reader is referred to the web version of this article).

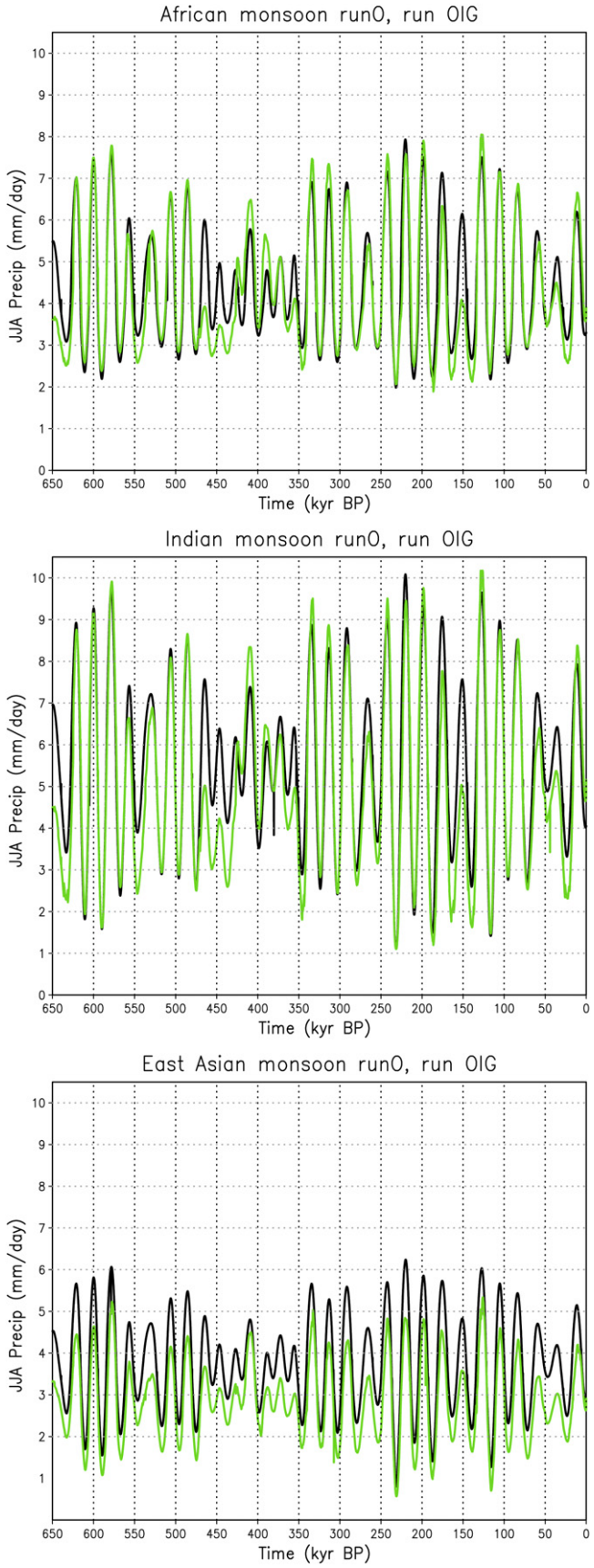

Fig. 3. JJA Precipitation for the African monsoon (top), Indian monsoon (middle) and East Asian monsoon (bottom) for run O (black) and run OIG (green). (For interpretation of the references to colour in this figure legend, the reader is referred to the web version of this article).

for periods between 40 and 42 kyr (obliquity). Filtering and computation of spectra was done with the Analyseries software (Paillard et al., 1996). We compute linear correlations, which seem adequate at the precession and obliquity bands in contrast to the 100 kyr timescale (Hargreaves and Abe-Ouchi, 2003).

3.1. The precession phase of boreal summer monsoons

The precipitation response to precession forcing is shown in Fig. 4. The spatial patterns are obviously only crudely resolved given the coarse resolution of the model. The figure gives the difference in the band-pass filtered data between arbitrarily chosen periods of precipitation minimum and maximum in the Indian monsoon. Patterns are similar in run O and run OIG, with slightly smaller response amplitude in the latter. This is also clear from the time-series of the Indian monsoon precipitation which is shown in Fig. 4 as well. Results are similar for the African and East Asian monsoon systems. At the precession period the correlation between monsoon precipitation and the orbital forcing is near-perfect, with a lag that is close to zero in run O (Table 1). In run OIG phase differences increase by 400 yrs at most. Differences between run O and run OIG are thus seen to be small.

In order to understand the small impact that variations in ice sheets and greenhouse gases have at the precession period, we next consider temperature variations. These strongly drive variations in monsoon precipitation, especially temperature variations over central Asia (Joussaume et al., 1999; Tuenter et al., 2003). Fig. 5 shows the spatial pattern of the temperature–precession correlation and the timing of the response in both experiments. Due to the absence of weather-like noise in CLIMBER-2, correlations are again near perfect in both runs. Temperature leads precession by 600–700 yr over central Asia in run O. This overall lead reflects the dominant control of May–June–July insolation on JJA temperatures, caused by the small thermal inertia of the land. In run OIG, lags are longer (by as much as 2–3 kyr), especially in gridboxes where ice sheets are located during glacial periods. However, over central Asia the impact of varying ice sheets and greenhouse gases is much smaller and lags increase by a few hundred years only.

3.2. The obliquity phase of boreal summer monsoons

Although obliquity mainly affects mid-high latitude insolation, there is a clear response of boreal summer monsoons to this remote forcing (Fig. 6). The figure gives the difference in the band-pass filtered data between arbitrarily chosen periods of precipitation maximum and minimum. Signals are weaker at the obliquity period than at the precession period, in agreement with earlier time-slice modelling results (Prell and Kutzbach, 1987; Tuenter et al., 2003). The Indian monsoon again shows the strongest response, while the African and East Asian monsoon signals are smaller and spatially varying. Signals can be stronger as well as weaker in run OIG compared to run O, depending on the location. Lags increase (Table 1). The longest lags are found in run OIG for the African and Indian monsoon systems, that are located closest to the Eurasian ice cap, while there is only a small shift in the phasing of the east Asian monsoon.

The temperature correlation (Fig. 7) reflects the spatial signature of the insolation forcing that is associated with obliquity, with a positive correlation at high latitudes (where the insolation forcing is positive for an obliquity maximum) and a smaller negative correlation in the tropics (were the insolation forcing is weaker). Lags are zero everywhere in run O. Inclusion of varying ice sheets and greenhouse gases in run OIG results in an increase in the lag by ca 5 kyr over the Eurasian ice sheet and in the subtropics, while the increase is smaller (2–3 kyr) over central

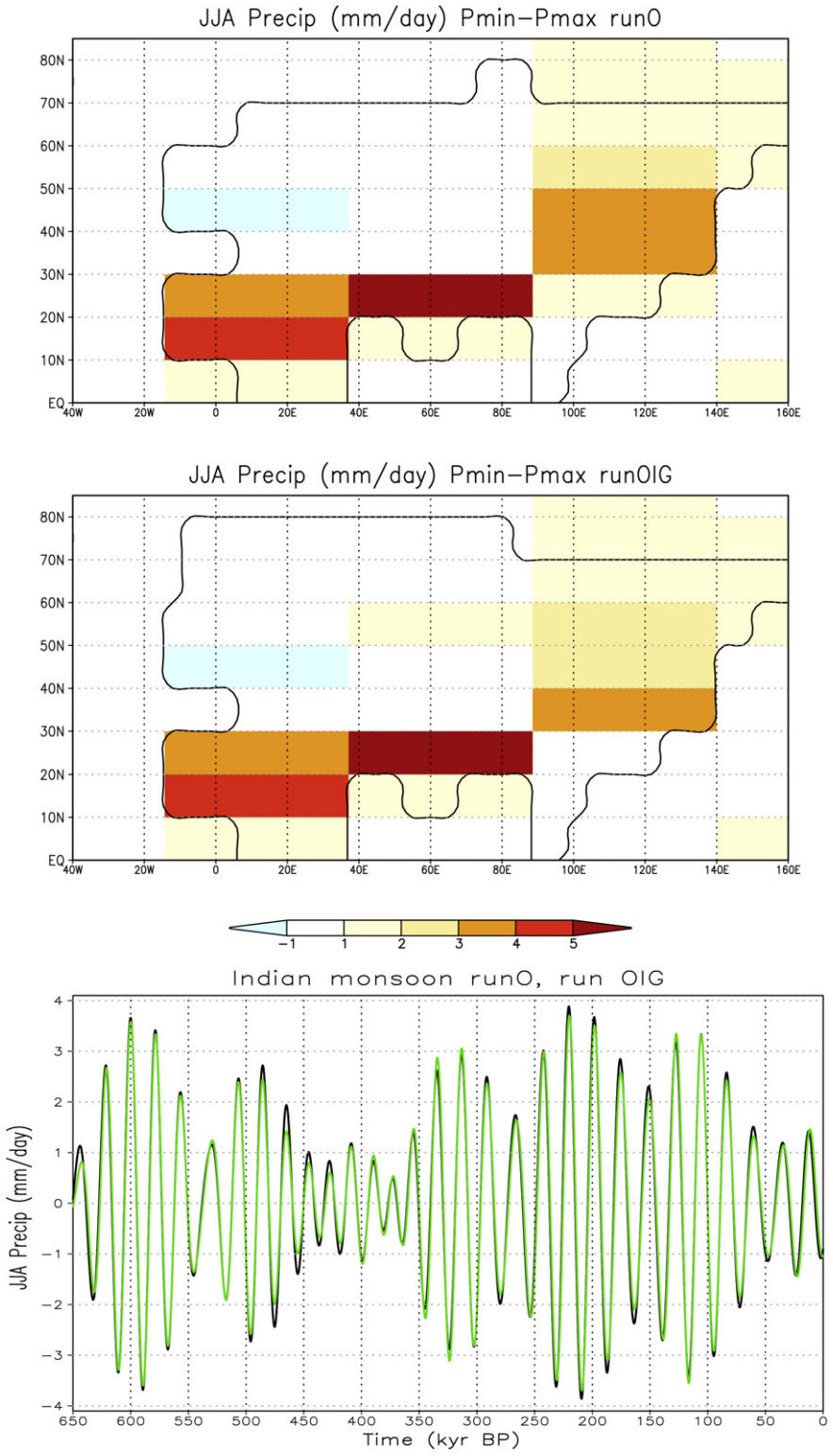

Fig. 4. Summer precipitation response to precession in the African/Asian region in run O (upper) and run OIG (middle), displayed on the CLIMBER-2 grid. Land contours are displayed at a finer resolution, which takes into account that a given grid cell can be partly land and partly ocean. Shown are the differences between periods of maximum precipitation of the Indian monsoon (at 600 kyr BP) and minimum precipitation (at 610 kyr BP). Timeseries of Indian monsoon precipitation (bottom), band-pass filtered for the precession period, in run O (black) and run OIG (green). (For interpretation of the references to colour in this figure legend, the reader is referred to the web version of this article).

Asia. Although ice sheets and greenhouse gases do have a clear impact at the obliquity band, correlations are still near perfect due to the high coherence between these additional forcings and the obliquity parameter.

3.3. Factor analysis and spectra

Monsoon variations in run OIG can be due to the orbital forcing, variations in ice sheets or greenhouse gases, or a combination of

Table 1
Correlation ρ and the lag L (in kyr) between simulated monsoon precipitation and the precession or obliquity parameter in run O (columns 2–3) and run OIG (columns 4–5). The last column gives the amplification factor A, defined as the regression coefficient in run OIG divided by the regression coefficient in run O. Precipitation lags the orbital parameters for positive lags with zero phase set at minimum precession and maximum obliquity, respectively.

Precession	ρ_O	L_O	ρ_{OIG}	L_{OIG}	A
Africa	0.997	−0.4	0.992	−0.1	0.95
India	0.997	−0.4	0.995	−0.1	0.97
East-Asia	0.997	−0.2	0.995	0.2	0.84
Obliquity					
Africa	0.952	0.5	0.961	2.9	1.67
India	0.951	0.1	0.958	2.5	1.35
East-Asia	0.950	0.1	0.944	1.3	0.88

these factors. In order to analyse the role of each forcing in more detail we apply the following regression model, where the simulated monsoon timeseries is expressed as:

$$M(t+L) = \alpha O(t) + \beta I(t) + \gamma G(t) + R \quad (1)$$

Here M is monsoon precipitation, O represents the orbital forcing (either the precession or obliquity parameter), I ice sheet area, G greenhouse gases and t time. The term R on the right-hand-side is added to statistically account for the possible inadequacy of the linear assumption applied here. It is assumed to be uncorrelated with the forcings. All terms are taken as anomalies with respect to the long-term mean, computed over the full simulation period. The lag L and regression coefficients α, β and γ are determined by a standard least-squares fitting procedure, which minimizes the distance between the simulated monsoon timeseries and the right-hand-side of (1) (the fitted timeseries). Results are given with I representing Eurasian ice sheet area variations. This was found to give slightly better results than when the American or the combined ice sheets are used. The 'goodness of fit, as quantified by the correlation (Table 2) between the fitted timeseries and the original timeseries that is simulated by the climate model, indicates that the linear regression performs well and that the R is negligibly small.

To quantify the contributions of each forcing factor (or combinations thereof) to the total variance Var_{tot} of the fitted monsoon timeseries obtained from (1), we derive the following relation:

$$Var_{tot} = \alpha^2 Var_O + \beta^2 Var_I + \gamma^2 Var_G + 2\alpha\beta Covar_{OI} + 2\alpha\gamma Covar_{OG} + 2\beta\gamma Covar_{IG} \quad (2)$$

Here *Var* denotes the variance and *Covar* the covariance of the variable(s) indicated in the subscript. The first three terms on the right-hand-side denote the contributions from the orbital forcing, ice sheets and greenhouse gases. The last three terms denote the contributions that arise from the coherent variations between the orbital forcing and ice sheets, the orbital forcing and greenhouse gases, and the ice sheets and greenhouse gases.

At the precession period almost all variance is due to the orbital forcing, with insignificant contributions from other factors (Table 2). This result is consistent with the small impact that was found in run OIG at the precession period from the inclusion of additional forcings.

At the obliquity period different factors play a role for the different monsoon systems. For the African and Indian monsoon varying ice sheets and greenhouse gases are important, as well as the covariance between them. For the East Asian monsoon orbital forcing is the dominant factor, with a smaller role for the coherent variations between ice sheets and greenhouse gases. The relative importance of these factors is also reflected in the lags by which each system responds to the orbital forcing at the obliquity period (Table 1). It is in-between to the ice-sheet lag of 7 kyr and the orbital lag of 0 kyr in case of the African and Indian monsoons and

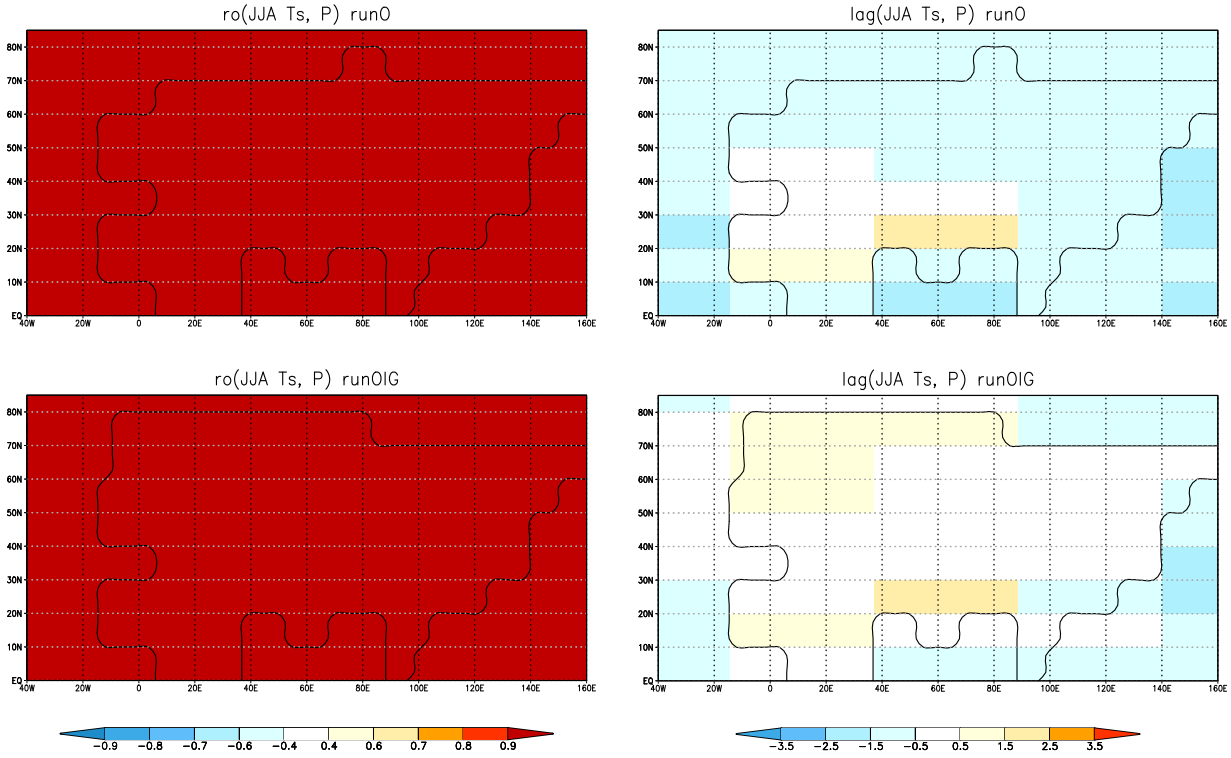

Fig. 5. Correlation (left) of summer temperature with precession and the lag (in kyr; right) at which the optimum correlation occurs. For negative lags temperature leads the precession parameter, with zero phase set at minimum precession (that is, maximum NH summer insolation). Upper panels give results from run O and lower panels from run OIG.

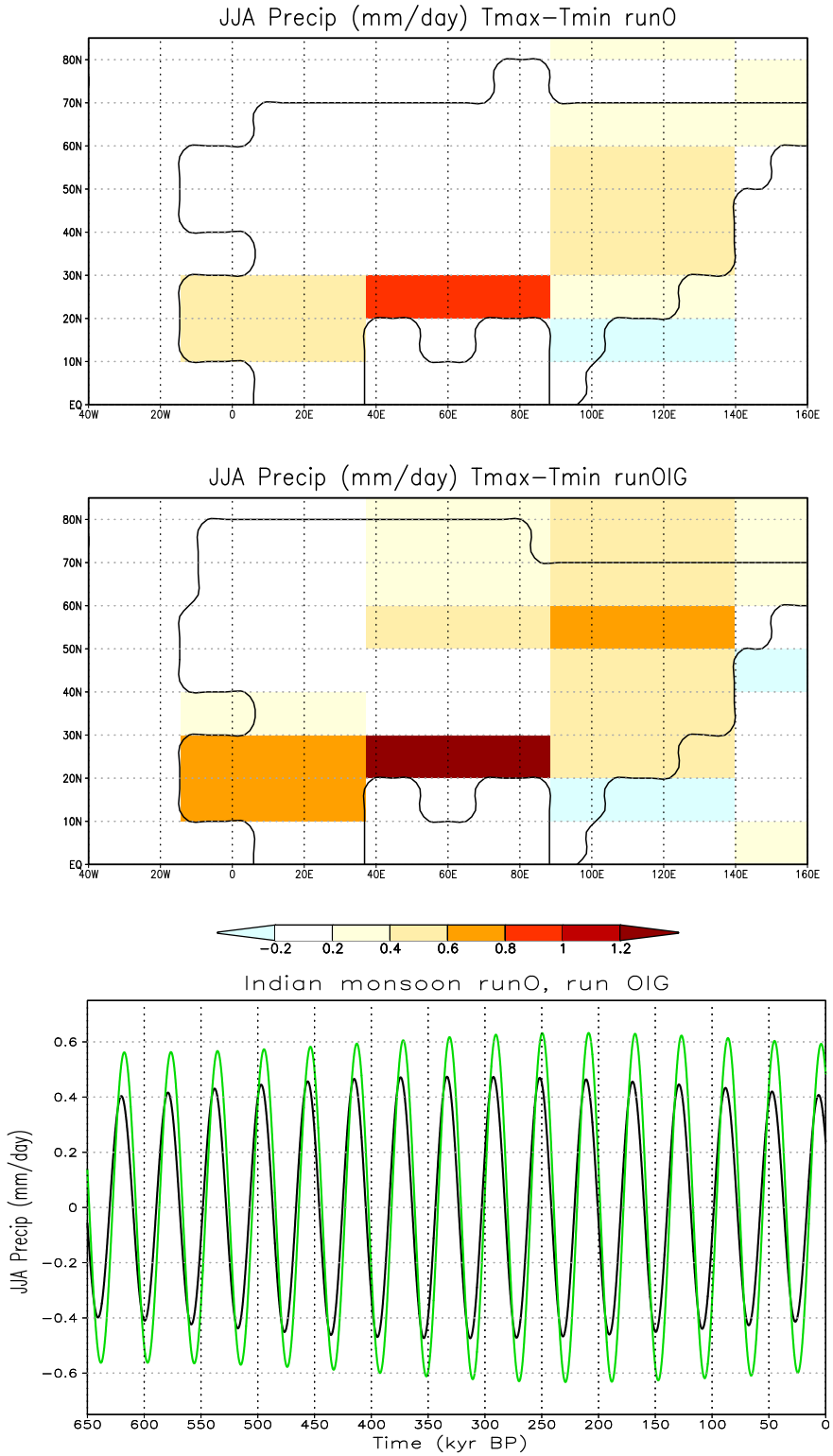

Fig. 6. Similar as Fig. 4 but now for the summer precipitation response to obliquity in run O (upper) and run OIG (middle). Shown are the differences between periods of maximum precipitation of the Indian monsoon (at 570 kyr BP for O and 250 kyr BP for OIG) and minimum precipitation (at 558 kyr BP for O and 270 kyr BP for OIG). Timeseries of Indian monsoon precipitation (bottom), band-pass filtered for the obliquity period, in run O (black) and run OIG (green). (For interpretation of the references to colour in this figure legend, the reader is referred to the web version of this article).

close to the lag associated with orbital forcing in case of the East Asian monsoon.

Finally we consider the spectra of monsoon precipitation (Fig. 8). In run O monsoon variance is strongly dominated by the precession timescale, with a subordinate influence of obliquity. There is no 100 kyr variance. Adding varying ice sheets and greenhouse gases in run OIG causes a small decrease of variance at the precession timescale. Precession remains dominant, but the

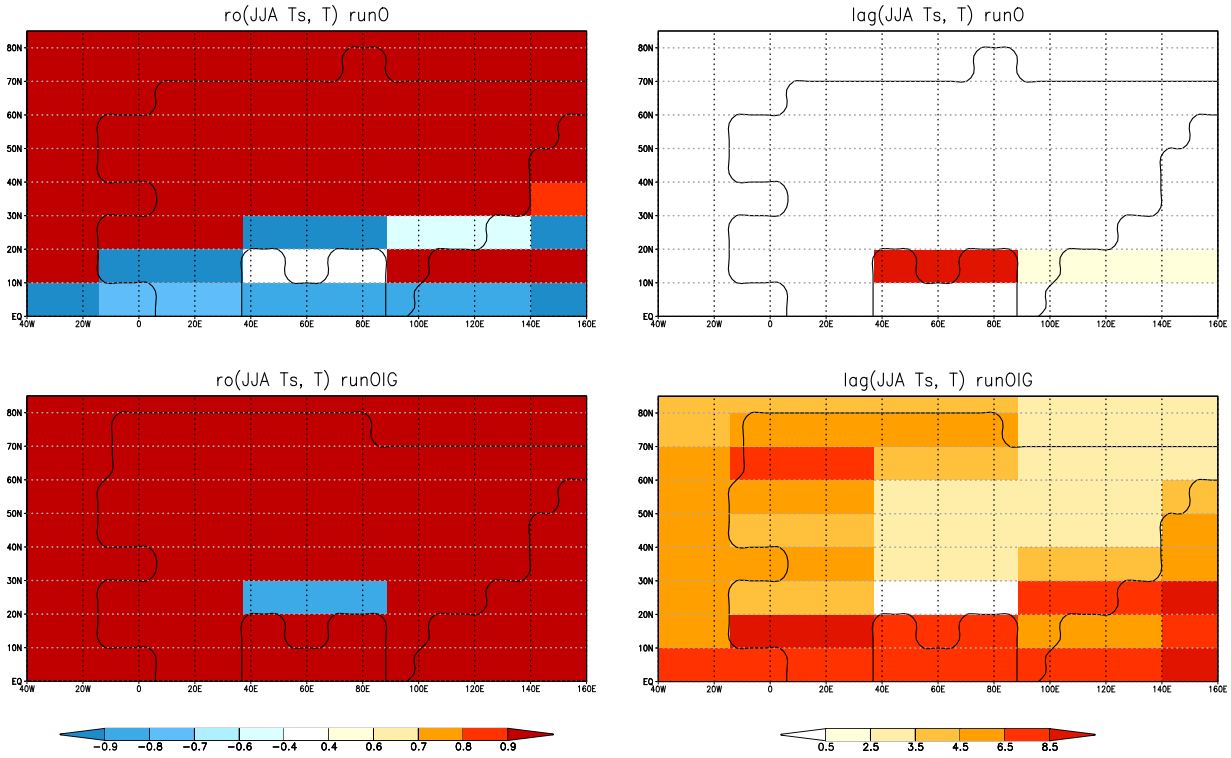

Fig. 7. Similar as Fig. 5, but now for obliquity. For positive lags temperature lags the obliquity parameter, with zero phase set at maximum obliquity (that is, maximum NH summer insolation).

ratio between the obliquity and precession peaks is larger in run OIG as compared to run O. In addition, there is a secondary peak at the 100 kyr period for the African and Indian monsoon systems due to ice and greenhouse gas variations.

4. Discussion

The impact of ice and greenhouse gases seems much smaller than one would expect, especially at the precession period. We not here that the general expectation of the impact of glacial boundary conditions is based on the LGM climate, that is, variations at the 100 kyr period. For the LGM CLIMBER-2 simulates a cooling over central Asia by 3–8 °C due to the presence of ice and by 2–3 °C due to the low greenhouse gas concentrations, in good agreement with results from more detailed, comprehensive GCMs (Schneider von Deimling et al., 2006). At the precession and obliquity periods variations in ice and greenhouse gases are much smaller. Consequently, they induce smaller variations in temperature (gradients) and thus in boreal summer monsoon systems.

An important caveat in the present study is the uncertainties associated with variations in ice sheet area. These can only be prescribed in a crude manner, given the coarse resolution of the climate model. In addition it is not clear how far east the Eurasian ice cap extended. The most recent reconstruction for the LGM, that was used as a reference here, shows no coverage over northwestern Siberia in agreement with pollen data for this region (Peltier, 2004). Use of this reconstruction in climate model simulations was found to give better agreement with data than an earlier reconstruction that extended more to the east (Kageyama et al., 2006). For this reason the present approach seems the best guess. Better constraints on the ice-sheet extent - also for earlier glacials - would considerably strengthen any assessment of the impact of ice-sheet variations.

A second caveat is the lack of atmospheric mid-latitude dynamics in the climate model used. This seems especially important for the East Asian monsoon, which shows little response to the glacial-age boundary conditions for all orbital periods. In a snapshot simulation it was found that the Eurasian ice sheet strongly influences the East Asian monsoon by generating a wave train that reinforces the monsoonal precipitation (Yin et al., 2009). Complex teleconnections associated with planetary waves were also found in other studies (for example, Hoskins and Rodwell (1995)). It seems therefore likely that the present results may change in some respects with increasing model resolution and sophistication. We view the present effort as a necessary first step in time-dependent modelling of late Pleistocene monsoon systems.

Data show varying lags at the precession period, as mentioned earlier. Different factors may play a role here. One factor is the seasonality of precession signals recorded in data (Kutzbach et al., 2008). Another factor may be that different climatic processes determine marine and terrestrial data (Ziegler et al., 2010).

Table 2
The correlation ρ between the fitted monsoon timeseries and the original timeseries, see Section 3.3. The following columns give the variance that is explained by each forcing factor (columns 3-5) and by the covariances between forcing factors (columns 6-8), all expressed as a percentage of the total variance of the original timeseries.

Precession	ρ	Orbital	Ice	GHG	Orb-Ice	Orb-GHG	Ice-GHG
Africa	0.992	98	0	0	1	0	0
India	0.994	98	0	0	0	0	0
East Asia	0.995	98	0	0	0	1	1
Obliquity							
Africa	0.997	0	34	17	2	2	44
India	0.996	1	26	22	3	5	43
East Asia	0.991	79	1	1	4	1	14

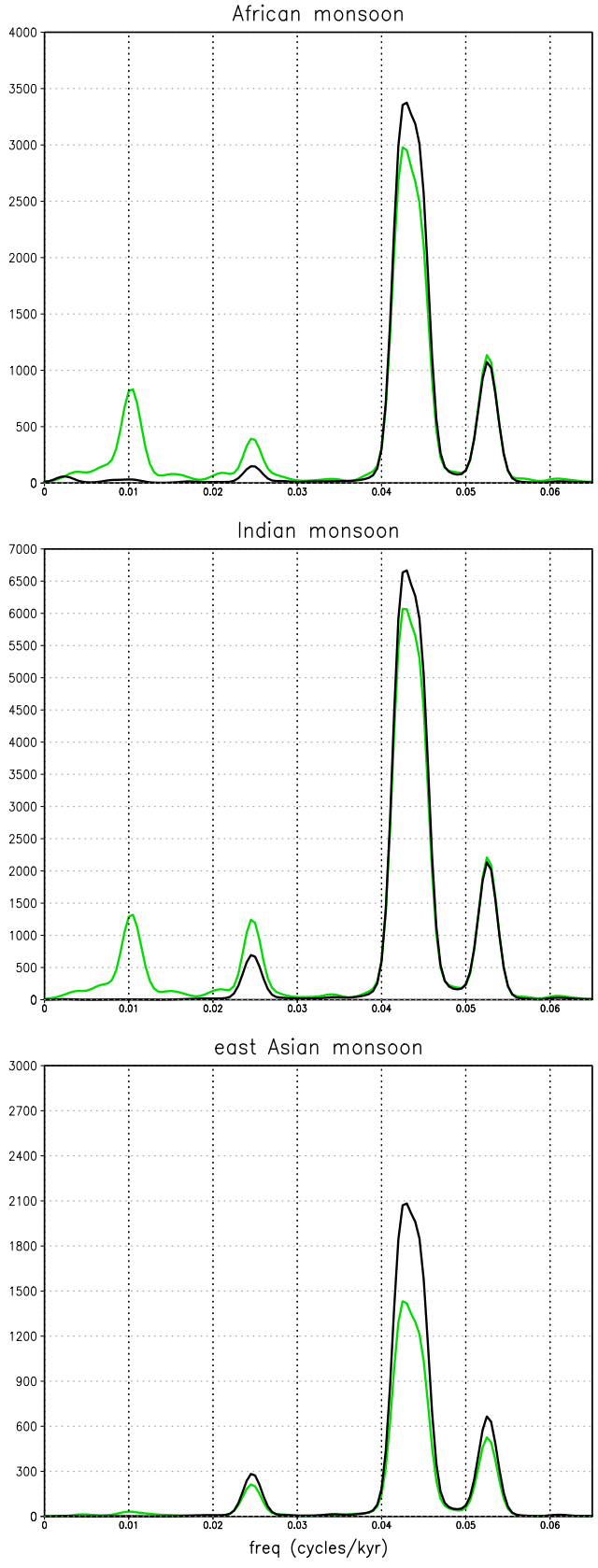

Fig. 8. Spectrum of monsoon precipitation in run O (black) and run OIG (green) for Africa (upper), India (middle) and East Asia (bottom). (For interpretation of the references to colour in this figure legend, the reader is referred to the web version of this article).

Unfortunately, the ocean circulation is too crudely resolved in the present study to examine this factor. Findings of Clemens et al. (2008) suggest an important role for ice volume, and latent heat export from the southern Indian Ocean at precession maxima, noting that the timing of the summer monsoons at the precession band changes from the Pliocene (small lags and little ice) to the late Pleistocene where the phase lags are large. Snap-shot sensitivity experiments seem to support this hypothesis (Liu et al., 2006). However, time-dependent experiments with the same GCM did not result in long lags at the precession period (Kutzbach et al., 2008). We conclude that the question of the timing of precession-forced boreal monsoons is as yet unresolved.

Model-data mismatches in lags may be due to a too simple interpretation of proxy records in terms of one climatic parameter only like summer monsoon precipitation. For example, modelling methane emissions in terms of different controlling processes resulted in a correct simulation of the lags in the measured methane record at both the precession and the obliquity periods (Konijnendijk et al., 2011).

The simulated obliquity phase of ca 3 kyr in the African and Indian monsoons is consistent with observational studies, which show boreal summer monsoon proxies to cluster between obliquity maxima (summer insolation maxima) and ice minima (Clemens et al., 2008). The absolute values of the lags simulated here depend on the timescales used in the forcing data, among other factors. Due to uncertainties in the age models, there are large uncertainties in the estimated lags (Mudelsee, 2001). The purpose of the present study has been to estimate monsoon lags using a well-tested climate model, given the most recent timescales, not to resolve the timescale problem itself.

5. Summary and conclusions

Time-dependent simulations for the period 650–0 kyr BP have been used to assess the impact of varying ice sheets and greenhouse gases on the intensity and timing of orbital-forced variations in boreal summer monsoons. We have found that the impact is small at the precession period, primarily resulting in a small reduction of monsoon variance but no shifts in the timing. Variations in the Eurasian ice cap are large enough at the precession period to have a local impact on surface air temperature. However, this does not affect monsoons which are primarily driven by summer temperature over the continental interior. The greenhouse gas forcing shows little power at the precession period. As a consequence, lags between boreal monsoons and the precession parameter are not affected by these additional forcings and remain close to zero whether they are included in the simulations or not.

At the obliquity period we find small increases in spectral power, but significant shifts in monsoon timing. Both land ice and greenhouse gases play a role, modifying surface air temperatures over large spatial scales. Monsoon variance over Africa and India is found to be largely controlled by ice-sheet variations, with a secondary influence from greenhouse-gas variations that are coherent with ice variations. Direct orbital forcing only contributes significantly to monsoon variance for East Asia. Lags vary from 3 kyr for the Indian and African monsoon systems, which are closest to the Eurasian ice sheet, to 1 kyr for the East Asian monsoon.

The presence of orbital cycles in many sedimentary records has been exploited to construct so-called astronomical timescales. This is done by statistical tuning of proxy data to an astronomical target curve, which contains the principal cycles in the orbital parameters. Significant lags are introduced for precession (4–5 kyr) and obliquity (7–8 kyr) if ice-age related proxies such as $\delta^{18}O$ are used for tuning (Imbrie et al., 1984; Lisiecki and Raymo, 2005). However, in case of Mediterranean sapropels, which reveal both the influence

of precession and obliquity, a much shorter lag of 3 kyr is assumed (e.g., Lourens et al., 1996, 2001). Our model results for the African monsoon, which is generally linked to those sapropel series, thus support the assumption of the Mediterranean sapropel-based astronomical timescale at the obliquity band, but leaves open the question of the mechanism underlying the lag as reconstructed at the precession band.

Acknowledgments

Thanks are due to Frits Hilgen, Lucas Lourens and Martin Ziegler for stimulating discussions. Andrey Ganopolski is thanked for his help in setting up the CLIMBER-2 experiments. Steve Clemens and Michel Crucifix are thanked for careful reading of the manuscript and their constructive reviews.

References

Braconnot, P., Loutre, M.-F., Dong, B., Joussaume, S., Valdes, P., PMIP participating groups, 2002. How the simulated change in monsoon at 6 ka BP is related to the simulation of the modern climate: results from the paleoclimate modeling intercomparison project. Climate Dynamics 19, 107–121.

Braconnot, P., et al., 2007. Results of PMIP2 coupled simulations of the mid-Holocene and last glacial maximum. Part 1: experiments and large-scale features. Climate of the Past 3, 261–277.

Bintanja, R., et al., 2005. Modelled atmospheric temperatures and global sea levels over the past million years. Nature 437, 125–128.

Claussen, M., et al., 1999. Simulation of an abrupt change in Saharan vegetation in the mid-Holocene. Geophysical Research Letters 26, 2037–2040.

Clemens, S.C., Prell, W.L., Sun, Y., Liu, Z., Chen, G., 2008. Southern hemisphere forcing of Pliocene $\delta^{18}O$ and the evolution of indo-Asian monsoons. Paleoceanography 23, PA4210. doi:10.1029/2008PA001638.

Clemens, S.C., Prell, W.L., Sun, Y., 2010. Orbital-scale timing and mechanisms driving late Pleistocene indo-Asian summer monsoons: reinterpreting cave speleothem $\delta^{18}O$. Paleoceanography 25, PA4207. doi:10.1029/2010PA001926.

Ganopolski, A., Rahmstorf, S., Petoukhov, V., Claussen, M., 1998a. Simulation of modern and glacial climates with a coupled model of intermediate complexity. Nature 391, 351–356.

Ganopolski, A., Kubatzki, C., Claussen, M., Brovkin, V., Petoukhov, V., 1998b. The influence of vegetation-atmosphere-ocean interaction on the climate during the mid-Holocene. Science 280, 1916–1919.

Ganopolski, A., Pethoukov, V., Rahmstorf, S., Brovkin, V., Claussen, M., Eliseev, A., Kubatzki, C., 2001. CLIMBER-2: a climate system model of intermediate complexity. Part II: model sensitivity. Climate Dynamics 17, 735–751.

Hall, A., Clement, A., Thompson, D.W.J., Broccoli, A., Jackson, C., 2005. The importance of atmospheric dynamics in the Northern Hemisphere wintertime climate response to changes in the Earth's orbit. Journal of Climate 18, 1315–1325.

Hargreaves, J.C., Abe-Ouchi, A., 2003. Timing of ice-age terminations determined by wavelet methods. Paleoceanography 19 (2), 1035.

Hoskins, B.J., Rodwell, M.J., 1995. A model of the Asian summer monsoon, Part I: the global scale. Journal of the Atmospheric Sciences 52, 1329–1340.

Imbrie, J., et al. (Eds.), 1984. Milankovitch and Climate, Understanding the Response to Astronomical Forcing, Part I. D. Reidel Publishing Company, Dordrecht/Boston/Lancaster, pp. 269–305.

Joussaume, et al., 1999. Monsoon changes for 6000 years ago: results of 18 simulations from the paleoclimate modeling intercomparison project (PMIP). Geophysical Research Letters 26, 859–862.

Kageyama, M., Laine, A., Abe-Ouchi, A., Braconnot, P., Cortijo, E., Crucifix, M., de Vernal, A., Guiot, J., Hewitt, C.D., Kitoh, A., Marti, O., Ohgaito, R., Otto-Bliesner, B., Peltier, W.R., Rosell-Mele, A., Vettoretti, G., Weber, S.L., Project Members, M.A.R.G.O., 2006. Last glacial maximum temperatures over the North Atlantic, Europe and western Siberia: a comparison between PMIP models, MARGO sea-surface temperatures and pollen-based reconstructions. Quaternary Science Reviews 25, 2082–2102.

Konijnendijk, T, Weber, S.L., Tuenter, E., and van Weele, M. Methane variations at orbital timescales, a transient modelling experiment. Climate of the Past Discussions, in press.

Kutzbach, J.E., 1981. Monsoon climate of the early Holocene: climate experiment with the earth's orbital parameters for 9000 years ago. Science 214, 59–61.

Kutzbach, J.E., Liu, X., Liu, Z., Chen, G., 2008. Simulation of the evolutionary response of global summer monsoons to orbital forcing over the past 280,000 years. Climate Dynamics 30, 567–579.

Laskar, J., Robutel, P., Joutel, F., Gastineau, M., Correia, A.C.M., Levrand, B., 2004. A long term numerical solution for the insolation quantities of the Earth. Astronomy and Astrophysics 428, 261–285.

Lisiecki, L., Raymo, M., 2005. A Pliocene–Pleistocene stack of 57 globally distributed benthic $\delta^{18}O$ records. Paleoceanography 20, PA1003. doi:10.1029/2004PA001071.

Liu, X., Liu, Z., Kutzbach, J.E., Clemens, S.C., Prell, W.L., 2006. Hemispheric insolation forcing of the Indian Ocean and Asian monsoon: local versus remote impacts. J. Clim 19, 6195–6208.

Loulergue, L., Schilt, A., Spahni, R., Masson-Delmotte, V., Blunier, T., Lemieux, B., Barnola, J.-M., Raynaud, D., Stocker, T.F., Chappellaz, J., 2008. Orbital and millennial-scale features of atmospheric CH4 over the past 800,000 years. Nature 453, 383–386. doi:10.1038/nature06950.

Lourens, L.J., Antonarakou, A., Hilgen, F.J., van Hoof, A.A.M., Vergnaud-Grazzini, C., Zachariasse, W.J., 1996. Evaluation of the Plio-Pleistocene astronomical timescale. Paleoceanography 11, 391–413.

Lourens, L.J., Wehausen, R., Brumsack, H.J., 2001. Geological constraints on tidal dissipation and dynamical ellipticity of the Earth over the past three million years. Nature 409, 1029–1033.

Lüthi, D., Le Floch, M., Bereiter, B., Blunier, T., Barnola, J.-M., Siegenthaler, U., Raynaud, D., Jouzel, J., Fischer, H., Kawamura, K., Stocker, T.F., 2008. High-resolution carbon dioxide concentration record 650,000–800,000 years before present. Nature 453, 379–382. doi:10.1038/nature06949.

Mudelsee, M., 2001. The phase relations among atmospheric co_2 content, temperature and global ice volume over the past 420 ka. Quaternary Science Reviews 20, 583–589.

Paillard, D., Labeyrie, L., Yiou, P., 1996. Macintosh program performs time series analysis. EOS 77, 379.

Peltier, W.R., 2004. Global glacial isostasy and the surface of the ice-age earth: the ICE-5G (VM2) model and GRACE. Annual Review of Earth and Planetary Sciences 32, 111–149.

Petoukhov, V., Ganopolski, A., Brovkin, V., Claussen, M., Eliseev, A., Kubatzki, C., Rahmstorf, S., 2000. CLIMBER-2: a climate system model of intermediate complexity. Part I: model description and performance for present climate. Climate Dynamics 16, 1–17.

Prell, W.L., Kutzbach, J.E., 1987. Monsoon variability over the past 150,000 years. Journal of Geophysical Research 92, 8411–8425.

Robertson, A., Overpeck, J., Rind, D., Mosley-Thompson, E., Zielinski, G., Lean, J., Koch, D., Penner, J., Tegen, I., Healy, R., 2001. Hypothesized climate forcing time series for the last 500 Years. Journal of Geophysical Research 106, 14,783–14,803.

Schneider von Deimling, T., Ganopolski, A., Held, H., Rahmstorf, S., 2006. How cold was the last glacial maximum? Geophysical Research Letters 33, L14709. doi:10.1029/2006GL026484.

Shine, K.P., Derwent, R.G., Wuebbles, D.J., Morcrette, J.-J., 1990. Radiative forcing of climate. In: Houghton, J.T., Jenkins, G.J., Ephraums, J.J. (Eds.), Climate Change, the IPCC Scientific Assessment. Cambridge University Press, Cambridge USA.

Tuenter, E., Weber, S.L., Hilgen, F.J., Lourens, L.J., 2003. The response of the African summer monsoon to remote and local forcing due to precession and obliquity. Global and Planetary Change 36, 219–235.

Tuenter, E., Weber, S.L., Hilgen, F.J., Lourens, L.J., Ganopolski, A., 2005. Simulation of climate phase lags in response to precession and obliquity forcing and the role of vegetation. Climate Dynamics 24, 279–295.

Wang, P., Clemens, S.C., Beaufort, L., Braconnot, P., Ganssen, G., Jian, Z., Kershaw, P., Sartnheim, M., 2005. Evolution and variability of the Asian monsoon system: state of the art and outstanding issues. Quaternary Science Reviews 24 (5–6), 595–629.

Wang, Y., Cheng, H., Edwards, R.L., Kong, X., Shao, X., Chen, S., Wu, J., Jiang, X., Wang, X., An, Z., 2008. Millennial-and orbital-scale changes in the East Asian monsoon over the past 224,000 years. Nature 451, 1090–1093. doi:10.1038/nature06692.

Yin, Q.Z., Berger, A., Crucifix, M., 2009. Individual and combined effects of ice sheets and precession on mis-13 climate. Climate of the Past 5 (2), 229–243.

Ziegler, M., Lourens, L.J., Tuenter, E., Hilgen, F., Reichart, G.-J., Weber, S.L., 2010. Precession phasing offset between Indian summer monsoon and Arabian Sea productivity linked to changes in Atlantic overturning circulation. Paleoceanography 25, PA3213. doi:10.1029/2009PA001884.